URN (Paper): urn:nbn:de:gbv:ilm1-2011iwk-105:6

56TH INTERNATIONAL SCIENTIFIC COLLOQUIUM
Ilmenau University of Technology, 12 – 16 September 2011
URN: urn:nbn:gbv:ilm1-2011iwk:5

TRUE 3D MEASUREMENTS OF MICRO AND NANO STRUCTURES

G. Dai, S. Bütefisch, F. Pohlenz, H.-U. Danzebrink, J. Fluegge

Physikalisch-Technische Bundesanstalt (PTB), 38116 Braunschweig, Germany

ABSTRACT

True 3D measurements of micro and nano structures remains challenging issues today. A newly developed 3D-AFM for true 3D measurements of nano structures and an ultra precision micro/nano CMM based on a nano measuring machine (NMM) for true 3D measurements of micro and millimetre size structures have been introduced in the paper. In the design of the 3D-AFM, the AFM probe is oscillated by two piezo actuators driven at vertical and/or torsional resonant frequencies of the cantilevers. This enables the AFM tip to probe the surface with a vertical and/or a lateral oscillation, offering high 3D probing sensitivity. The instrument can be operated in different modes: static, vertical oscillation, torsional oscillation, and combined vertical and torsional oscillation modes by configuring the driven signals in different ways. In addition, a so called "vector approach probing" (VAP) method is applied for enhancing the measurement flexibility and minimising the tip wear. Some preliminary experimental results using the vertical oscillation mode are demonstrated, showing very promising performance. The measurement of a IVPS 100 sample employing a flared AFM tip is performed, showing a repeatability of its 3D profiles of better than 1 nm (p-v). A single crystal critical dimension reference material (SCCDRM) having features with almost vertical sidewalls is measured using a flared AFM tip. Results show that the feature has averaged left and right sidewall angles of 86.1° and 86.8°, respectively. However, the feature width non-uniformity may reach 10 nm within the measurement range of 1 µm. The standard deviation of the averaged middle CD values of 22 repeated measurements reaches 0.3 nm. In addition, an investigation of long term measurement stability is performed on a PTB photomask. The results change with a rate of about 0.00033 nm per line, which confirms the high measurement stability and the very low tip wear. In the developed micro/nano CMM, two kind of tactile probes are applied: a piezoresistive probe and an ACP ball probe. Its probing repeatability reaches 1.3 nm, 4.4 nm and 4.4 nm along the x, y and z axes, respectively. Calibration of micro/nano NMMs remains a critical issue. A novel 3D test artefact fabricated using the wet etching technique is introduced, which can be applied to characterise the 3D geometric properties of micro/nano CMMs with only one measurement.

Index Terms – micro/nano dimensional metrology, true 3D measurements, 3D AFM, Critical Dimension (CD), micro/nano CMM

1. INTRODUCTION

Quantitative dimensional measurements of micro- and nano structures are increasingly demanded due to the rapid developments in, for instance, semiconductor industry, precision engineering industry, microsystem technology and materials science. The sizes of the nano- and micro structures range from nanometres to hundreds of micrometres, while the measurement tasks can be categorised as one dimensional (1D), two dimensional (2D), two and half dimensional (2.5D) and true three dimensional (3D) measurements.

Various techniques are available today for measuring micro and nano structures, however, most of them are not true 3D techniques. Optical and scanning electron microscopes are 2D techniques only. Although further techniques such as phase shifting interference microscopes, white light scanning microscopes and confocal microscopes are able to provide 3D views of structures, they are not true 3D techniques since they are lacking of capabilities in measuring steep sidewalls of structures. True 3D measurements of micro and nano structures remain challenging issues today.

In this paper, developments at PTB for true 3D measurements of micro and nano structures will be presented. In order to perform true 3D measurements of nano structures, a 3D-AFM with vertical and torsional oscillation modes has been recently developed. And for performing true 3D measurements of micro and millimetre size structures, a micro/nano CMM has been built up based on an accurate nano positioning/measuring machine (NMM)[1].

2. DEVELOPMENT OF A 3D-AFM FOR TRUE 3D MEASUREMENTS OF NANO STRUCTURES.

2.1. Instrumentation

The developed 3D-AFM applies conventional conical or pyramidal shaped AFM tips for measuring structures with non-steep sidewalls, and flared AFM tips for measuring structures with steep sidewalls. It is able to measure in both static and dynamic modes. Its working principle is shown in figure 1. The cantilever, mounted to an alignment chip (not shown), is oscillated by two shaking piezos, SP_1 and SP_2. By applying a sinusoidal driving signal Sd_v with a frequency near the cantilever's vertical (flexure) resonant frequency, the two shaking piezos are excited in phase and consequently a vertical oscillation of the tip can be generated. By applying a sinusoidal driving signal Sd_t with a frequency near the cantilever's torsional resonance frequency, the two shaking piezos are excited out of phase and consequently a torsional oscillation of the cantilever can be generated, which leads to a horizontal oscillation of the AFM tip. By applying the driving signals Sd_v and Sd_t simultaneously, the AFM tip can be oscillated with a trajectory consisting of both the vertical and horizontal motions.

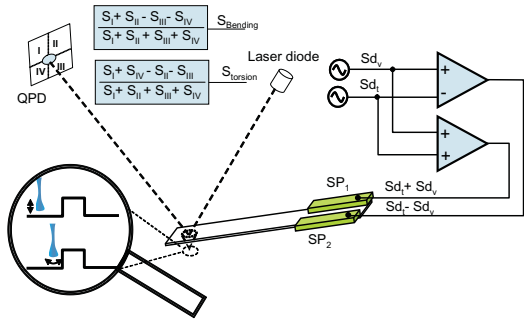

Fig.1 Principle of 3D-AFM head with vertical and torsional oscillation modes.

When a structure with steep sidewalls is measured using a flared AFM tip in the 3D-AFM, the vertical oscillation of the tip can be applied to probe its top and bottom regions, while the horizontal oscillation of the tip can be employed to probe its sidewalls, as shown in the inset of figure 1. In such a way, the whole structure can be detected by the tip oscillated in a direction normal to its surface, offering high 3D probing sensitivity. As a contrast, in conventional AFMs the cantilever is usually driven by one shaking piezo and oscillates in the vertical direction only. This mode is principally not ideal for sensing vertical sidewalls since the tip oscillates almost parallel to the surface being measured, i.e. the tip-sample distance does not change within the oscillation cycles. Consequently, the tip sample interaction force such as van der Waals force changes little during the oscillation cycles, which may impact the probing sensitivity.

The 3D-AFM applies a classical optical lever technique to detect the bending and torsion of the cantilever. The beam from a laser diode is focused on the backside of the cantilever and is received by a quadrant photodiode (QPD) after being reflected. The vertical (bending) and torsional signals of the cantilever, Sv and St, can be obtained by processing the signals from the QPD. The Signals S_v and S_t are processed by two lock-in-amplifiers (LIAs) which use the signals driving the excitation piezos Sd_v and Sd_t as the reference signals, respectively, yielding amplitude and phase signals (A_v, P_v and A_t, P_t). The signals A_v , P_v and A_t , P_t together with S_v and S_t are analog to digital converted under the synchronization of the positioning signals of motion stages. All signals are further real time processed in a digital signal processing (DSP) system for measurements.
The 3D-AFM is capable of measuring in four different probing modes by configuring the driving and measurement signals in different ways:

- Static mode where both driving signals Sd_t and Sd_v are switched off and the detection signals S_v, S_t are applied for measurements.
- Vertical oscillation mode where the driving signal Sd_t is switched off while Sd_v is on. The tapping amplitude and phase signals A_v , P_v are used for measurements.
- Torsional oscillation mode where the driving signal Sd_t is switched on while Sd_v is off. The torsional amplitude and phase signals A_t, P_t are employed for measurements.
- Combined vertical and torsional oscillation mode where both Sd_t and Sd_v are switched on. The amplitude and phase signals of the tapping and/or torsion oscillations (A_v, P_v and A_t, P_t) are applied for measurements.

When working in the dynamic modes, the cantilever of the 3D-AFM is oscillated near its vertical and/or torsional resonant frequencies. The resonant frequencies are determined by frequency tuning of the cantilever. For the AFM probe type CDR120 (http://www.team-nanotec.de/), for instance, we had measured its torsional resonant frequency of around 1.8 MHz with a Q factor of about 800, and a vertical resonant frequency of around 260 kHz with a Q factor of about 400. A photo of the developed 3D-AFM is shown in figure 2.

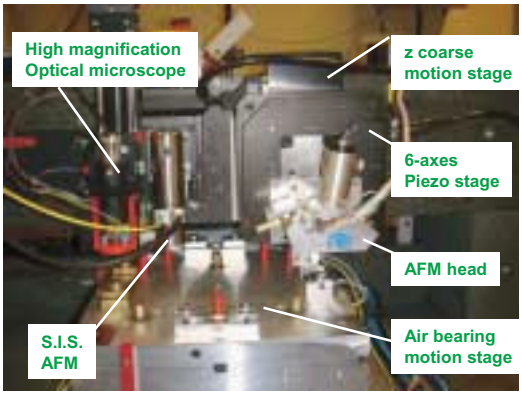

Fig.2 Photo of the 3D-AFM

The 3D-AFM is operated in the scanning head principle. It has the advantage that large samples (for instance, wafers and photomasks) can be kept stationary while the 3D-AFM head is moved during AFM measurements. A commercial 6-axes nano positioning stage (type P-561K034, Physik Instrumente GmbH) is applied for moving the AFM head. The nano positioning stage is a flexure hinge stage driven by piezo actuators with its positions and angles measured and servo controlled based on high resolution capacitive sensors. The geometrical scaling factors of the 3D-AFM are calibrated to the PTB metrological large range AFM [2] via a sets of step height and lateral standards. The measurement range of the 3D-AFM is 15 µm × 45 µm × 45 µm (x, y, z). An air bearing stage with a travel range of 550 mm x 300 mm is applied for coarse positioning of the sample. For reducing the vibration noise, the air bearing is deactivated so that the motion table is set down before the AFM measurement starts.

2.2. Probing and Measurement strategy

In order to minimize the tip wear and enhance the measurement flexibility, a so-called "vector approaching probing" (VAP) [3] method is implemented in the 3D-AFM. The VAP method is similar to a step-in measurement method proposed in [4], and the difference is that the "VAP" method can work both in contact and dynamic modes. Using the VAP method, the structure is measured point by point. At each measurement point, the tip is moved towards the surface until the desired tip-sample interaction is detected and then immediately withdrawn from the surface. The probing direction is usually set to be normal to the surface for achieving highest probing sensitivity, however, other probing directions are also allowed. The VAP method is capable of measuring vertical or even reentrant sidewalls.

A VAP measurement process consists of three phases as shown in figure 3(a). The first is the approaching phase. In this phase, the tip is moved towards the surface at a desired probing velocity v_p (for instance 500 nm/s ~ 1000 nm/s) and the tip sample interaction is monitored in real time. The first phase ends once the tip sample interaction reaches a pre-defined status ST_1. The second is the probing phase. In this phase, the tip is moved towards the surface until another pre-defined status ST_2 is reached. Then the tip is withdrawn immediately from the surface until the tip sample interaction reaches again the status ST_1. During the second phase, the x, y and z position of the nano positioning stage and the probe signals of sample interaction are recorded in real time and stored in the buffer of the DSP system. The third is the positioning phase. In this phase, the tip is moved to the next measurement point. The time needed for a complete VAP process is approximately $2d_{t\text{-}s}/v_p$, where $d_{t\text{-}s}$ is the initial tip sample separation before the VAP starts.

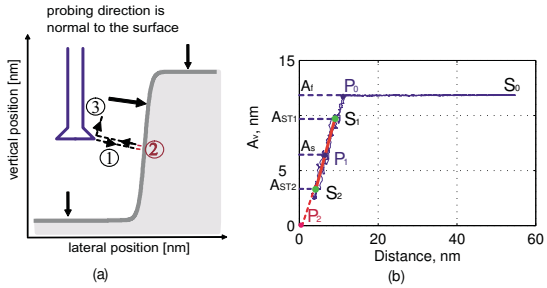

Fig.3 Principle of the "vector approach probing" is shown in (a) and a typical probing curve is shown in (b).

The tip-sample interaction mentioned above is a general term, and may have different meanings for different measurement modes. For instance, in static measurement mode it is indicated by the static bending and torsion of the cantilever. In vertical oscillation mode, the vertical oscillation amplitude and phase are taken as tip sample interaction signals. In torsional oscillation mode, the torsional oscillation amplitude and phase are applied instead. While in combined vertical and torsional oscillation mode, it is represented by the amplitude and phase signals of both vertical and torsional oscillations.

A typical probing curve measured using the VAP method is shown in figure 3 (b) as an example. The curve is recorded in measuring a horizontal surface by a tip probing in the vertical direction using the vertical oscillation mode during all three probing phases. The free oscillation amplitude of the tip A_f is about 12 nm. Before the VAP process starts, the tip has a tip-sample distance of about 50 nm plotted as the point S_0. After the probing starts, the tip is approached towards the surface until it reaches the point P_0. During this period of time, the oscillation amplitude A_v changes little, because the tip is far from the surface and the tip-sample interaction force is almost zero. At the position P_0, the tip-sample interaction becomes significant and A_v starts to decrease. The approaching phase ends at the point S_1 where $A_v = A_{ST1}$ and enters the probing phase. In the probing phase, the tip is further moved towards the surface and A_v decreases. The motion is stopped at the point S_2 where $A_v = A_{ST2}$ and then the tip starts to withdraw from surface until the point S_1 is reached again. In the third probing phase, the tip is moved back to its original position which is shown as the segment $S_1P_0S_0$ in the curve. After the probing curve is taken, a line is fitted to the data points between the point S_1 and S_2 , and the surface position can be calculated as the point P_1 ($A_v = A_s$) on the fitted line.

It is to be mentioned that the values A_{ST1}, A_{ST2}, and A_s are configurable by the user. Actually the configuration of A_s is related to the fundamental question of the measurement: How is the boundary of the surface defined? Therefore, for achieving the best

measurement performance, the same set of configuration parameters should be applied both when the 3D-AFM is measuring unknown samples and when it is calibrated using a known reference material. In addition, the probing curve may appear non-linear due to, for instance, the "snap-in" of the tip to the surface during measurement. In our study, we set the driving frequencies of the cantilever slightly below its resonance frequencies. This measure is able to improve the linearity of the probing curve according to our simulation results of the tip sample interaction force and the cantilever's dynamic response. Moreover, the values A_{ST1}, A_{ST2} are set so that a linear part of the probing curve is used for data evaluation.

In order to achieve high probing sensitivity, the tip should approach and probe the sample in a direction normal to its surface. However, this needs the prior knowledge about the form and the position of the structure. Unfortunately, for the very first profile such prior knowledge does not exist. Therefore, a measurement strategy for measuring the very first profile in three steps was designed. First, the structure is measured using the VAP method with a fixed probing direction, for instance, vertically. Second, the measurement profile is fitted to several segments. The measurement strategy allows that each segment being individually configured, for instance, how many measurement points should be taken, which measurement mode should be applied, etc. Third, the structure is measured again with a probing direction normal to its surface, referred to as the 3D probing strategy in context.

When the following profiles are to be measured, the previously measured profile can be applied as the prior knowledge, from which the measurement strategy for the next line can be adopted automatically. It is based on the fact that the profile of a (line) structure at different positions are usually alike. In addition, this measurement strategy can self-adapt to unavoidable measurement drift automatically, since the fresh measured data are always applied to generate the new measurement strategy.

The VAP method has two major advantages. Firstly, it offers more flexibility in measurements. The surface is measured point by point using the VAP method, which allows the flexible definitions of the measurement points. The part of the structure which is more important for the measurand can be measured in more detail. For instance, in measuring the middle CD the sidewalls of structure can be measured with higher pixel density than at the bottom and the top. In such a way, the number of measurement points can be greatly reduced, reducing the measurement time and minimizing the tip wear. Furthermore, the probing direction, probing velocity, and probing mode at different measurement points can be configured appropriately in the software. This allows each point be measured individually for optimizing the measurement performance. In addition, the measured coordinate at each point is evaluated from a recorded tip-sample interaction curve rather than coordinates of a point. Such a tip-sample interaction curve provides more information for data processing. Secondly, compared to the conventional scanning AFM where the tip is kept continuously in interaction with the surface, the tip sample interaction time using the VAP method is greatly reduced and consequently the tip wear can be reduced.

However, the VAP method has the disadvantage of a relative long measurement time. To overcome this drawback, a high-end DSP system is applied in our design where the tip-sample interaction is recorded and processed in real-time in the DSP, and only the evaluated result (the coordinates of the surface points) are transferred to the host computer. In such a way, the time needed for data transfer is greatly reduced. In the current design, a measurement speed of typically 3 ~ 20 points/sec can be achieved, depending on the selected probing parameters.

In addition to the VAP method which is specially designed for true 3D measurements, the 3D-AFM is also capable of performing scanning in the same way as a classical AFM, where a conical or pyramidal shaped tip is raster scanned with respect to the sample in the x, y plane while the tip sample interaction is kept constant by servo controlling the z position of the tip.

2.3. Measurement results

A number of measurements have been performed to investigate the capability and performance of the developed 3D-AFM. In this section, some selected results taken on a IVPS 100 sample, a SCCDRM sample, and a PTB photomask are focused.

To demonstrate the imaging capability of the 3D-AFM, an AFM image measured on a sample with GaN nanorods is shown in figure 4(a) with a cross sectional profile at the marked position shown in figure 4(b).

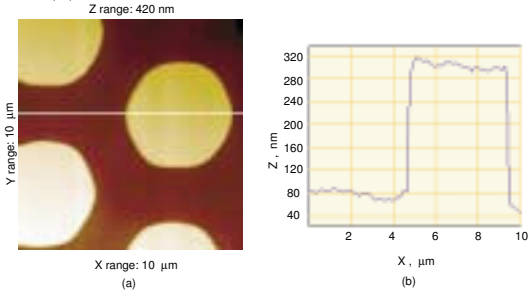

Fig.4 An AFM image measured on a sample with GaN nanorods is show in (a) with a cross sectional profile at the marked position in (b).

A sample type IVPS 100 from the company team nanotech has been measured for testing the capability of the 3D-AFM in measuring the true 3D form of structures. The sample contains silicon lines with vertical, parallel sidewalls (111-crystal planes). The

features have a nominal depth of 900 nm and a nominal sidewall angle 90°. In this investigation, a used flared AFM tip type CDR130s has been applied in the vertical oscillation mode. Since the feature depth is larger than the length of the applied CDR tip, a designed software function called "virtual cut-off plane" is applied which limits the tip to measure only the upper part of the feature for protecting the tip. Five profiles at the same position were taken with the slow scan axis being disabled for testing its measurement stability. The measured profiles are shown in figure 5, with three insets showing the details at three marked areas selected at the left sidewall, top and right sidewall regions, respectively. The profiles shown are the measured raw data without data smoothing or filtering, but including the dilation effects of the tip shape. It can be seen that the instrument can resolve the 3D form of the structure with a repeatability of better than 1 nm (p-v).

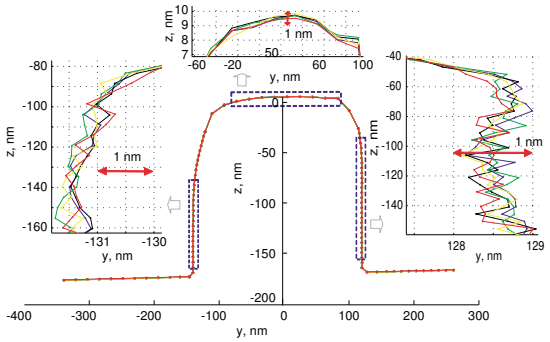

Fig.5 Measured profile of a IVPS 100 sample with the insets showing the details at the marked areas. Five profiles repeatedly measured are shown in the figure.

A SCCDRM sample [5] developed at the National Institute of Standards and Technology (NIST) of the United States has been measured by the developed 3D-AFM. The sample has a size of approximately 1 cm x 1 cm x 1 mm. The top surface of the standard is comprised of a number of patterns, many of them consisting of six line features of different widths ranging from 30 nm to 250 nm, as shown in figure 6 (a). The measurement area is precisely selected by using the alignment markers. The measurement is performed by a new flared AFM tip type CDR120 in the vertical oscillation mode. The driving frequency is set at a frequency slightly below the vertical resonance frequency of the cantilever. The structure is probed at a velocity of 1000 nm/s. An overview 3D-AFM image of the five structures are shown in figure 6(b), and a cross sectional profile is shown in figure 6(c). Note that the 6th structure was not measured due to a defect at the line feature.

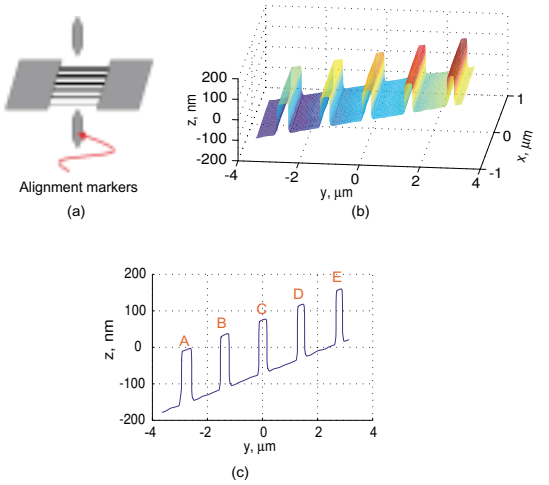

Fig.6 Layout of linewidth features of a single crystal critical dimension reference material (SCCDRM) is shown in (a), an overview 3D-AFM image of five line features in (b), and a cross sectional profile (c). The shown profile includes the dilation effects of the tip width.

Individual structures of the SCCDRM samples are measured using the 3D probing strategy. The measurement area is set to be about 0.8 µm × 1.0 µm. The profile is measured with 50 points at the left bottom, left sidewall, top, right sidewall and right bottom regions each, and with 5 points at the left-down, left-top, right-top and right-bottom corner regions each. One complete profile contains 270 measurement points. Sixteen profiles have been taken in one measurement run, which takes about 20 minutes. A 3D view of the measured linewidth feature B is shown in figure 7(a), and a typical cross-sectional profile is shown in figure 7(b) as the raw data without data smoothing or filtering. The inclination of the profile is linearly fitted and removed. To evaluate the middle CD value, part of the profile at the left and right bottom regions and at the top region (marked in red) are selected for calculating the structure height, H. It should be mentioned that the distance from the profile part to the structure corner should be properly selected (one-third of the line width in this study) so that the corner rounding regions of the structure are excluded. For achieving better statistic performance, the part of the left and right sidewall profiles within the z range of 0.3*H and 0.7*H are linearly fitted, respectively, as shown in figure 7(c) and (d). The sidewall positions are calculated as the intersection points between the fitted sidewall lines with the middle height line. The middle CD is evaluated as the distance between sidewall positions. The slopes of the fitted sidewall profiles are calculated as the slopes of the sidewalls.

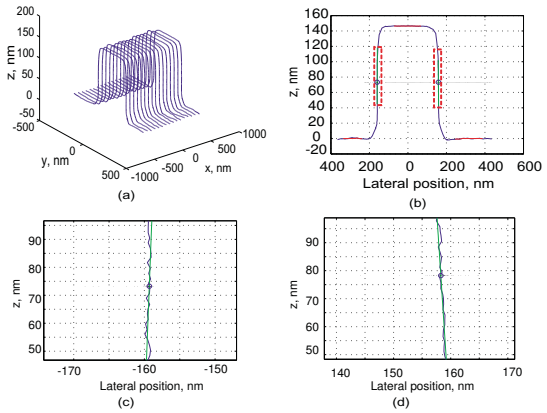

Fig.7 3D view of the measured linewidth feature B is shown in (a), a cross-sectional profile of the feature is shown in (b), the left and right sidewalls of the feature are zoomed-in and shown in (c) and (d).

Calculated middle CD values of 16 profiles of 22 repetitive measurements are shown in figure 8. It can be seen that the structure has different CD values with a variation of up to 10 nm at different profile positions due to the non-uniformity of the feature width. However, the CD values measured at the same profile position repeat well. The mean CD value of a measurement is calculated as the averaged result of CD values of 16 profiles. The standard deviation of the mean CD values of 22 repetitive measurements reaches 0.3 nm showing the static repeatability of the instrument

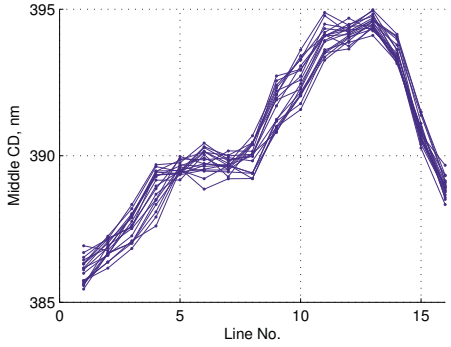

Fig. 8 Measured middle CD values on different profiles in 22 repeated measurements using vertical oscillation mode. (The given CD values include the effective tip width.)

The left and right sidewall slopes calculated from 16 profiles of 22 repetitive measurements are shown in figure 9 (a) and (b), respectively. The determined slope values have a standard deviation of about 0.2°, which can be attributed to the sidewall roughness and the measurement noise. The averaged values of the left and right sidewall slopes are 86.1° and 86.8°, respectively, indicating that the sidewalls of the SCCDRM features are nearly vertical.

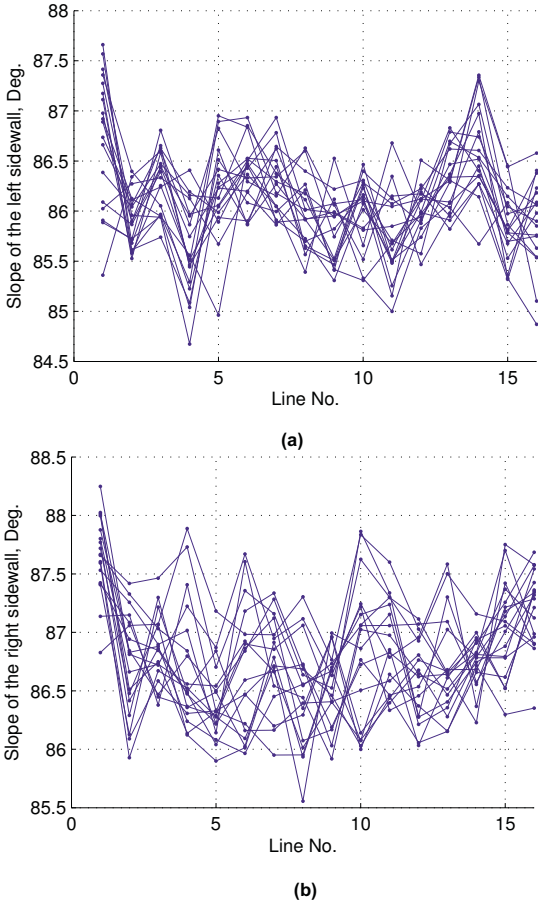

Fig. 9 Measured left and right sidewall slopes of structure B in 22 repeated measurements

An investigation on the long term stability of the 3D-AFM has been performed by measuring a PTB photomask having the material of Cr on quartz. A line feature with a nominal width of 300 nm has been measured within an area of 750 nm × 1000 nm in vertical oscillation mode using the 3D probing strategy. Before the measurement started, a new AFM probe with flared tip type CDR120 has been mounted. All measurement data have been recorded and evaluated, therefore, the tip wear even from the very first measurement could be monitored. The whole investigation lasted about 30 hours during a weekend. A total 197 measurements have been performed with each taking about 9 minutes. The whole measurement is run fully automatically without any operator's interaction once the measurement task was defined and started. The measured middle CD values are plotted in figure 11. It can be seen that the variation of the middle CD changes less than 1 nm. By linearly fitting the measured values shown as the red line in the figure, the changing rate is determined as approximately 0.00033 nm per line. This result indicates that the 3D-AFM has a very high measurement stability and very low tip wear.

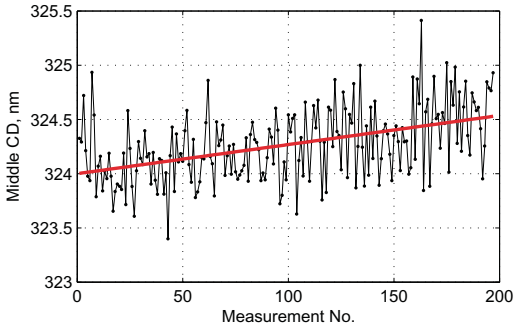

Fig.10 Long term stability in CD measurements using vertical oscillation mode. (The given CD values include the effective tip width.)

3. DEVELOPMENT OF A MICRO/NANO CMM FOR TRUE 3D MEASUREMENTS OF MICRO AND MILLIMETRE SIZED STRUCTURES

Our development of the micro/nano CMM based on a NMM has been published elsewhere [6], therefore, it will be introduced very briefly here for the completeness of the paper.

3.1. Instrumentation

In the developed CMM, the sample to be measured is moved by the NMM along the x, y and z axes. To enhance the dynamic performance of the NMM, an xyz piezo positioning stage is to be coupled to the NMM, which could help to realise fast CMM scanning functions. The sample is probed by two kinds of tactile micro/nano CMM probes: a 3D piezoresistive micro probe [7] and an assembled cantilever ball probe (ACP ball probe). A home-designed software has been applied for carrying out CMM measurements. Besides, a more specific commercial CMM software (Quindos 7.0, Messtechnik Wetzlar GmbH) has additionally been coupled to the instrument to allow flexible measurements and data evaluations of complex components. A photo of the developed instrument is shown in figure 11.

Fig.11 Photo of the micro/nano CMM based on the NMM

The piezoresistive probe is based on a boss membrane made from single crystalline silicon by means of anisotropic etching. As shown in the figure 12(a), the fabricated sensor chip includes a centre boss, a membrane with a thickness of tens of micrometers and a frame. On this chip a shaft with a length of about 10 mm is glued to the centre boss, and a probing sphere with a diameter of some hundred micrometers is glued to the free end of the shaft using the glue UHU plus endfest 300 (UHU GmbH). The probe was originally designed and fabricated at the Institute for Micro Technology of the TU Braunschweig [7]. The photo of such a sensor chip is shown in figure 12(b).

Four groups of piezoresistive sensors arranged as Wheatstone bridges are fabricated on the backside of the membrane by focused ion-beam doping technique and act as sensor elements. When the probing sphere touches the measurement object, strains are produced on the membrane by the probing force, which lead to changes of the resistances of the piezoresistive sensors. Finite Element Analysis (FEA) method has been used during probe design to calculate the position where the maximum strains occur. At these positions, the piezoresistive sensors are located for optimum measurement sensitivity, as shown in figure 12(c). The resistance changes of the sensors are converted to electrical signals which are used to determine the probe's displacement, i.e. for measurement.

Besides the piezoresistive 3D micro CMM probe, an ACP ball probe has also been developed in our study. The structure and measurement principle of the ACP ball probe are shown in figure 13. The probe consists of an scanning force microscope (SFM) cantilever, on which a shaft is mounted. A probing ball located at the free end of the shaft is used to probe the object to be measured. The whole probe is fixed to a substrate plate, which can be oscillated by a dither piezo in dynamic mode.

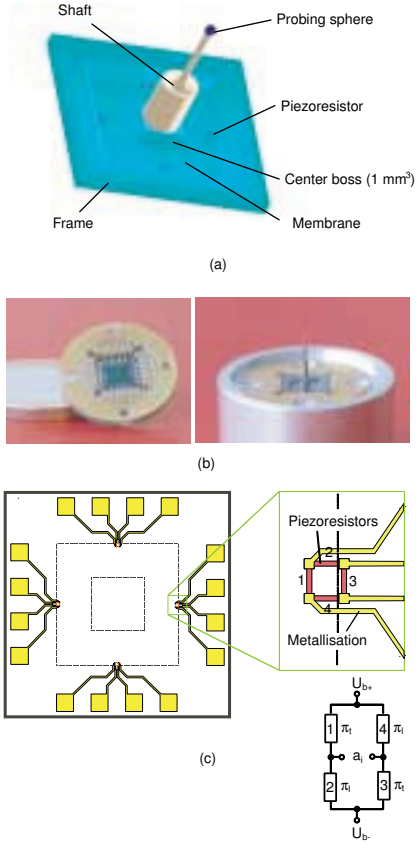

Fig. 12 The 3D structure of the piezoresistive micro CMM probe is shown in (a). The photos of the fabricated sensor chip and the micro 3D CMM probe as a whole are demonstrated in (c), where an one euro coin is given for illustrating the size of the probe. The layout of the piezoresistance sensors (Wheatstone bridges) at the back side of the membrane is illustrated in (b).

The measurement principle of the ACP probe is straightforward and similar to a classical AFM probe, namely that the bending and/or torsion of the cantilever will be changed as well as the oscillation of the cantilever will be damped when the probing ball touches the object's surface. By detecting the motion of the cantilever with the optical lever method the sample-probe interaction is measured. As an example, typical probing curves are shown in figure 14 (a). The measured point, P, is calculated as the "zero force" probing point as shown in figure 14(b). In addition, the slopes of the probing curves S_1 and S_2 can be used to determine the probing direction.

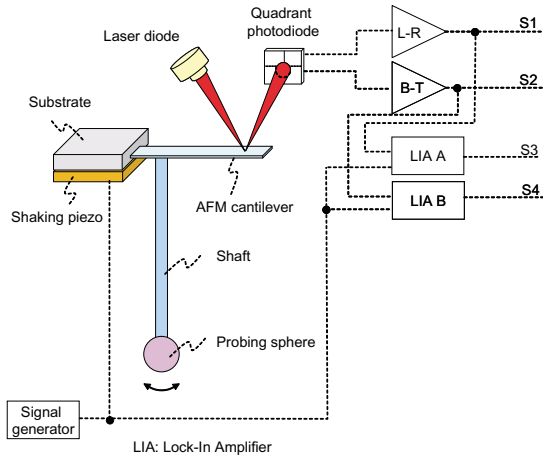

Fig.13 Measurement principle of the ACP ball probe

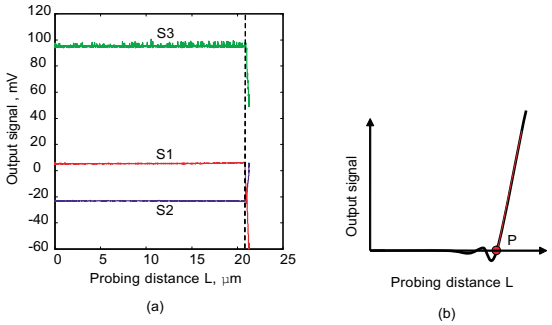

Fig.14 Typical probing curves of the ACP ball probe are shown in (a) and the method to determine the zero force probing point P is shown in (b)

The developed micro/nano CMM is capable of 3D measurement with nanometer accuracy. As shown in figure 15, the probing repeatability is demonstrated where the CMM is commanded to measurements at the same position of the sample. The standard deviations of results are 1.3 nm, 4.4 nm and 4.4 nm along the x, y and z axes, indicating the good measurement performance of the system. The piezoresistive probe is applied in this investigation, however, the ACP probe also show similar performance.

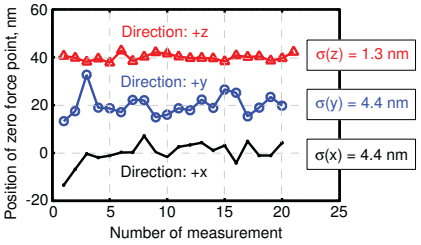

Fig.15 Measured probing repeatability along the x, y and z-axis.

More measurement applications were demonstrated in publications [6,8].

3.2. Calibration of Micro/nano CMMs

With the increasing developments of micro/nano CMMs, the calibration of these devices becomes an important issue, for instance, the calibration of the form of the probing sphere, the probe stiffness, and the geometric errors of the motion stage.

The form of the probing sphere can be conveniently calibrated by applying a reference sphere will known (small) form error. However, for ultra precision CMM, the form deviation of the reference sphere will be a major uncertainty contribution. To overcome this problem, Küng et al. had implemented a three-spheres calibration method based on the error separation techniques [9].

The probing force of a micro/nano CMM should be in the milli- or micronewton range to avoid plastic deformations. And it is desired that the probe has equal stiffnesses in any probing direction. Calibrations of spring constants of micro/nano CMM probes in all three probing directions using reference springs are introduced in [10].

Concerning the calibration of the geometric errors of the motion stage, 1D/2D/3D artefacts such as ball bars, ball arrays and ball plates are widely used for mapping the stage errors in conventional CMMs. However, they are inconvenient in use, since they have to be measured in different orientations in order to map the full 3D measurement volume of micro/nano CMMs, or sometimes such calibrations are even not possible due to the mechanical interference between the artefact and the probing head. We proposed therefore a novel 3D test artefact. The layout of such an artefact is shown in figure 16. It consists of several pyramidal structures having a size of 6.5 x 6.5 x 1.6 mm³. The pyramidal structure has four plateaus. On each plateau, there are small micro marks fabricated. The micro marks have also four sided pyramidal shape with a size of hundreds of micrometres. The corner angle of the micro mark is 109.4° (2 times 54.7°), defined by the orientation of the silicon crystal planes.

Each mark represents a point in 3D space, whose 3D coordinates can be calibrated using metrological instruments and used as the reference coordinates. When a micro/nano CMM is characterised using this type of artefact, the geometrical errors of the CMM will lead to a distortion of the 3D coordinates of the micro marks in its measured results. By evaluating the measured 3D coordinates and its reference coordinates, the 3D geometrical errors of the CMM can be calculated.

The 3D test artefact offers several advantages in calibrating micro/nano CMMs. Firstly, it is a 3D test artefact, which is capable of characterising the 3D geometric properties of micro/nano CMMs with only one measurement. Secondly, it can be mass fabricated using the well developed wet-etching technique with very low cost. However, there are also challenging issues existing, for instance, the quality of the micro mark which may strongly impacts the calibration performance.

(a) (b)

Fig. 16 Layout of the 3D test artifact for micro/nano CMMs is shown in (a), and a photo of a wafer of such artefacts fabricated using photolithography based micromachining techniques is shown in (b) [11].

A preliminary methods for calibrating the 3D test artefact have been developed [11]. Using this method, the centre of the mark is roughly determined by probing the four pyramid sides of the micro mark at first. Then the micro mark is centralised with respect to the CMM probe, and the contours of pyramid sides in the xz and yz planes can be measured by probing at different heights. After linear fitting the contours, the position of the micro mark can be calculated from the intersection position of the fitted lines.

Fig. 17 shows the static measurement repeatability of such a pyramidal structure. Totally 67 marks have been measured in this structure, and the deviations between two repeated measurements are plotted. It can be seen that the reproducibility is mostly within +/- 15 nm.

However, it should be stressed that the reproducibility shown above is the static repeatability. The performance becomes worse after the artefact being remounted due to the quality issue of the micro mark. Further investigations are to be carried out.

4. CONCLUSION

True 3D measurements of micro and nano structures remain challenging issues today. This paper introduced a newly developed 3D-AFM for true 3D measurements of nano structures. In its design, the AFM probe is oscillated by two piezo actuators driven at vertical and/or torsional resonant frequencies of the cantilevers. This enables the AFM tip to probe the surface with a vertical and/or a lateral oscillation, offering high 3D probing sensitivity. The instrument can be operated in different modes: static, vertical oscillation, torsional oscillation, and combined vertical and torsional oscillation modes by configuring the driven signals in different ways. In addition, a so called “vector approach probing” (VAP) method is applied for enhancing the measurement flexibility and minimising the tip wear. Some preliminary experimental results using the

vertical oscillation mode are demonstrated, showing very promising performance. In addition, an ultra precision micro/nano CMM based on a NMM is introduced for true 3D measurements of micro to millimetre size structures. Two kind of tactile probes: a piezoresistive probe and an ACP ball probe are applied to the developed CMM. Finally, calibrations of micro/nano CMMs have been discussed, and a novel test artefact has been introduced.

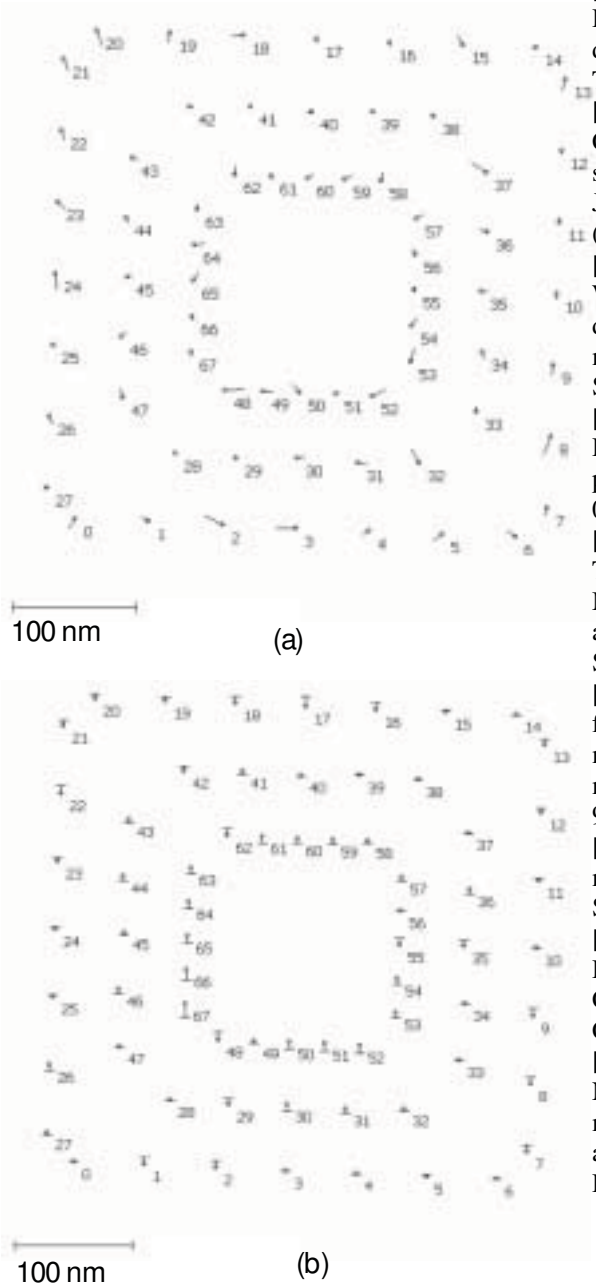

Fig. 17 Deviation of two repeated measurements of the 3D test artifact, shown as (a) lateral deviations and (b) vertical deviations.

5. REFERENCES

[1] G. Jäger, E. Manske, T. Hausotte, H.J. Büchner, Nanomessmaschine zur abbefehlerfreien Koordinatenmessung, Technisches Messen, 67, 319-23 (2000)

[2] G. Dai, H. Wolff, F. Pohlenz and H.-U. Danzebrink, A metrological large range atomic force microscope with improved performance, Rev. Sci. Instrum. 80, 043702 (2009)

[3] D. Hüser, W. Häßler-Grohne, K.-D. Katzer, J. Hunecken, H.-A. Fuß, H. Bosse, Kraftmikroskopie durch Einzelpunktantastung an Strukturkanten, Technisches Messen 77, 583 (2010)

[4] K. Murayama, S. Gonda, H. Koyanagi et al. Critical-dimension measurement using multi-angle-scanning method in atomic force microscope, Japanese Journal of Applied Physics, 45, 5928-5932. (2006)

[5] R. G. Dixson, R. A. Allen, W. F. Guthrie, and M. W. Cresswell, Traceable calibration of critical-dimension atomic force microscope linewidth measurements with nanometer uncertainty. J. Vac. Sci. Technol. B 23, 3028-3032 (2005)

[6] G. Dai, S. Buetefisch, F. Pohlenz and H.-U. Danzebrink, A high precision micro/nano CMM using piezoresistive tactile probes, Meas. Sci. Technol. 20 084001 (2009).

[7] S. Bütefisch, S. Dauer, S. Büttgenbach, Silicon Three-Axial Tactile Sensor for the Investigation of Micromechanical Structures. 9th Intern. Trade Fair and Conf. for Sensors, Transducers & Systems, Proc. Sensors 99, Vol. 2, pp. 321-326, Nürnberg (1999)

[8] G. Dai, H. Wolff , H.-U. Danzebrink, Atomic force microscope cantilever based microcoordinate measuring probe for true three-dimensional measurements of microstructures, Appl. Phys. Lett. 91, 121912 (2007)

[9]A. Küng, F.Meli and R. Thalmann, Ultraprecision micro-CMM using a low force 3D touch probe, Meas. Sci. Technol. 18 319–327 (2007)

[10] G. Dai, S. Bütefisch, F. Pohlenz, U. Brand, H.-U. Danzebrink, H. Bosse, Characterisation of micro/nano CMM probes, Proceedings of the euspen International Conference – San Sebastian (2009)

[11] S. Bütefisch, G. Dai, H. U. Danzebrink et al. Novel calibration artefactsand tactile probesfor micro/nano-CMMs, 257th PTB Seminar: “3D Micro- and Nanometrology - Requirements and Current Developments”, Braunschweig (2010)